New Phytologist

Research

# Salt stress induces the formation of a novel type of 'pressure wood' in two *Populus* species

**Dennis Janz[1], Silke Lautner[2], Henning Wildhagen[3], Katja Behnke[4], Jörg-Peter Schnitzler[4], Heinz Rennenberg[3,5], Jörg Fromm[2] and Andrea Polle[1]**

[1]Forstbotanik und Baumphysiologie, Büsgen-Institut, Georg-August-Universität Göttingen, Göttingen, Germany; [2]Zentrum für Holzwirtschaft, Universität Hamburg, Hamburg, Germany; [3]Institut für Forstbotanik und Baumphysiologie, Albert-Ludwigs-Universität Freiburg, Freiburg, Germany; [4]Institute of Biochemical Plant Pathology, Research Unit Environmental Simulation, Helmholtz Zentrum München, Munchen, Germany; [5]King Saud University, Riyadh, Saudi Arabia

Author for correspondence:
*Andrea Polle*
*Tel: +49 551393480*
*Email: apolle@gwdg.de*

Received: *27 August 2011*
Accepted: *14 October 2011*

*New Phytologist* (2012) **194**: 129–141
**doi**: 10.1111/j.1469-8137.2011.03975.x

**Key words:** arabinogalactan protein, biomass, carbohydrate, fasciclin-like protein, phloem, salt transcriptome, wood, xylem.

## Summary

- Salinity causes osmotic stress and limits biomass production of plants. The goal of this study was to investigate mechanisms underlying hydraulic adaptation to salinity.
- Anatomical, ecophysiological and transcriptional responses to salinity were investigated in the xylem of a salt-sensitive (*Populus* × *canescens*) and a salt-tolerant species (*Populus euphratica*).
- Moderate salt stress, which suppressed but did not abolish photosynthesis and radial growth in *P.* × *canescens*, resulted in hydraulic adaptation by increased vessel frequencies and decreased vessel lumina. Transcript abundances of a suite of genes (*FLA*, *COB-like*, *BAM*, *XET*, etc.) previously shown to be activated during tension wood formation, were collectively suppressed in developing xylem, whereas those for stress and defense-related genes increased. A subset of cell wall-related genes was also suppressed in salt-exposed *P. euphratica*, although this species largely excluded sodium and showed no anatomical alterations. Salt exposure influenced cell wall composition involving increases in the lignin : carbohydrate ratio in both species.
- In conclusion, hydraulic stress adaptation involves cell wall modifications reciprocal to tension wood formation that result in the formation of a novel type of reaction wood in upright stems named 'pressure wood'. Our data suggest that transcriptional co-regulation of a core set of genes determines reaction wood composition.

## Introduction

Soil salinity is a worldwide problem. Salt-affected soils cover a total area of 397 million ha, nearly 3% of the total land mass (FAO, 2006). Of this area, 77 million ha comprise agricultural land. The land fraction lost for farming because of soil salinity will increase in the coming years as a result of inappropriate irrigation and effects of global warming (Kundzewicz *et al.*, 2007). Research on salt-tolerance mechanisms in plants has been intensive, but mainly focused on agricultural crops or the model plant Arabidopsis (Amtmann & Sanders, 1999; Munns & Tester, 2008). To date, wood is gaining importance as a renewable resource. Sustainable woody biomass production on marginal or degraded soils in areas afflicted by salt or drought is desirable because this may contribute to solving the conflict of land use for either bioenergy or food production. For tree improvement toward increased stress tolerance, in-depth understanding of tree adaptation to salinity is required. Basic cellular defense mechanisms such as activation of the salt overly sensitive (SOS) pathway and antioxidative systems to prevent cellular injury are similar in tree and herbaceous species, but trees, which persist for many years on salt-affected sites, need additional protective measures to maintain growth and wood production (Chen & Polle, 2010).

A hallmark of woody lifestyle is the formation of a tall stem that supplies the crown with water and mineral nutrients. Osmotic stresses such as salinity and drought diminish radial growth and change xylem anatomy (Chen & Polle, 2010; Fischer & Polle, 2010). Ecophysiological studies in woody species along a gradient from humid to arid conditions showed that vessel diameters are inversely related to vessel numbers (Sperry *et al.*, 2008; Teichmann *et al.*, 2008). Woody species share a basic construction principle for drought adaptation that results in cell wall reinforcement by increasing wall thickness relative to lumen area while avoiding excess loss in water conductance by increasing vessel numbers. Recent studies with *P.* × *canescens* showed that this relationship also holds for the composition of the hydraulic system within one genotype (Arend & Fromm, 2007; Kundzewicz *et al.*, 2007; Beniwal *et al.*, 2010) and points to environmental sensing that enables flexible adjustment of xylem anatomy to osmotic conditions.

The molecular mechanisms leading to adaptive modifications in xylem anatomy of trees exposed to high salinity are not yet clear. Growth reductions may be the result of decreases in photosynthetic activity, leading to a lack of photosynthates (Kozlowski, 1997; Escalante-Perez *et al.*, 2009) or decreases in the K : Na ratio, leading to a lack of potassium (Langer *et al.*, 2002; Escalante-Perez *et al.*, 2009) or changes in hormone concentrations, especially reductions in auxin and increases in ethylene concentrations affecting xylem anatomy (Junghans *et al.*, 2004, 2006; Teichmann *et al.*, 2008). It is unknown if adaptation of the hydraulic system to salt stress results in modification of chemical wood composition.

The aim of the present study was to link transcriptional responses to salt stress with anatomical and chemical changes in the xylem of the secondary growth zone. We compared non-stressed and salt-stressed plants of the salt-sensitive *P.* × *canescens* with the salt-tolerant *Populus euphratica*. We measured transcriptional profiles of developing xylem tissue, wood anatomy and composition, element content, osmotic potential, net $CO_2$ assimilation rates and phloem sugar contents to disentangle the influence of carbohydrate supply, ion imbalances and osmotic disturbance on the hydraulic system.

## Materials and Methods

### Plant material, growth conditions and stress treatment

Plantlets from *P.* × *canescens* (*P. alba* × *P. tremula*) clone INRA717 1-B4 (Leplé *et al.*, 1992) and *P. euphratica* clone B2 from the Ein Avdat valley in Israel (Brosché *et al.*, 2005) were multiplied by *in vitro* micropropagation (Rutledge & Douglas, 1988) and kept in aerated hydroponic culture using Long Ashton nutrient solution (Hewitt & Smith, 1975), which was changed weekly. Plants were grown in a climatized chamber at 26°C, with a relative air humidity of 60% and a 16 : 8 h, light : dark cycle with photosynthetic active radiation (PAR) of 150 μmol $m^{-2}$ $s^{-1}$ (fluorescent lamps: L58W/25 and 58W/840, Osram, Munich, Germany; and TLD 58W/840 Philips, Amsterdam, the Netherlands). After 8 wk plants of each species were divided into three groups, of which one received 25 mM NaCl in the nutrient solution for 2 wk. Subsequently the salt-acclimated group was exposed for 2 wk to 100 mM NaCl and the second group to 25 mM NaCl. The third group served as an unstressed control. Each group consisted of 24 individual plants, and all 144 plants were harvested at the end of the 12 wk period. Plant height and stem diameter 2 cm above the root neck (digital caliper) were recorded regularly.

### Harvest of plant material

Mature leaves were sampled from the middle third of the plant, that is, from 0.2 to 0.4 m for *P.* × *canescens* and from 0.3 to 0.6 m for *P. euphratica*. Stem samples were taken from a height of 0.05 m above the root–stem junction. Whole roots were also harvested. The developing xylem was defined as all extraxylary tissue obtained by scraping the surface of the xylem with a razor after removal of the bark (as described by Teichmann *et al.*, 2008). Samples were directly frozen in liquid nitrogen and kept at −80°C. For anatomical analysis, samples were fixed in FAE (2% formaldehyde, 5% acetic acid, 63% ethanol). For DW, osmolyte content, Fourier transform infrared (FTIR) spectroscopy and element analysis, samples were dried in an oven (Memmert, Schwabach, Germany) at 70°C for 7 d, or at 105°C for 5 d (osmolyte content).

### Anatomy and histochemistry

Cross-sections (20 μm thick) were obtained using a sliding microtome. Cuttings were stained for 6 min with astra blue (0.1% astra blue, w/v), washed and stained for 2 min with safranine (0.1% safranine, w/v), then washed and mounted on glass slides. Sections were viewed under a light microscope (Axioskop, Zeiss) using ×250 magnification. Photographs were taken with a digital camera (Axiocam, Zeiss). Morphometric measurements (cell lumina and cell number) were carried out in newly formed wood tissue in the outer 100 μm of the xylem of stem cross-sections using ImageJ (Abramoff *et al.*, 2004). The predicted hydraulic conductivity was calculated as $\sum r^4$ $mm^{-2}$.

The pH in the developing xylem was determined by soaking fresh debarked stem segments for 2 min in 0.02% toluylene red solution. The stem segments were dried at room temperature and photographed with a DSLR camera (Pentax *ist DL2). CMYK color values were digitally measured in ImageJ (Abramoff *et al.*, 2004) and calibrated with a pH series. The pH series was prepared by adding 0.2 ml 0.2% toluylene red solution to 1.8 ml of water whose pH had been adjusted by NaOH and HCl. pH values were determined with a pH meter (pH meter pH526, WTW, Weilheim, Germany).

### Element distribution by EDX-SEM

After freeze-drying, stem cross-sections were coated with chromium and examined on a scanning electron microscope (AMR 1200, Leitz), equipped with an energy dispersive x-ray (EDX) microanalysis system (KEVEX 4000). Element-specific X-ray spectra were obtained from the developing xylem using a reduced scan raster area at ×500 magnification. Relative element concentrations were expressed as peak : background values from 24 recorded spectra.

### Osmolyte content and element analysis

Osmolyte content was measured in samples of leaves, stem, developing xylem and roots. Dried samples were milled (Retsch, Haan, Germany). Fifty micrograms of powder were incubated in 2 ml reaction tubes with 1.5 ml $H_2O$ at 55°C overnight. Samples were centrifuged at 100 ***g*** for 25 min. Fifty microliters of the supernatant were analyzed in a cryoscopic osmometer (Osmomat 030, Gonotec, Berlin, Germany). Using dry and fresh mass measurements, osmolyte concentrations were calculated. Osmotic potential was estimated using the van't Hoff law $\Psi = -RTc$, where $\Psi$ is the osmotic potential in Pa, $R$ = 8.314 $JK^{-1}$ $mol^{-1}$, $T$ the absolute temperature in K, and $c$ the solute concentration in mol $l^{-1}$.

For element analysis, tissue powder was pressure-extracted in $HNO_3$ (Heinrichs *et al.*, 1986). Elements were measured by inductively coupled plasma-optical emission spectrometry (ICP-OES; Spectroflame, SPECTRO Analytical Instruments, Kleve, Germany).

### Photosynthetic gas exchange

Gas exchange rates were measured using a portable gas exchange fluorescence system (GFS-3000 Walz, Effeltrich, Germany). Leaves (numbers 9 or 10 below the apex) were dark-adapted for 30 min, subsequently exposed for 30 min to light (1000 µmol PAR $m^{-2}$ $s^{-1}$ and 30°C leaf temperature) and then gas exchange parameters were averaged for 5 min.

### Carbohydrate content of phloem exudates by HPLC

Phloem exudates of bark pieces were collected as described in Rennenberg *et al.* (1996). Phloem exudate (1 ml) was mixed with 20 mg of polyvinylpolypyrrolidone (PVPP), shaken continuously for 1 h at 4°C, and centrifuged at 12 000 ***g*** for 10 min at 4°C. The supernatant was diluted with one volume of deionized water. An aliquot of 100 µl of the diluted supernatant was injected into a high-performance liquid chromatography (HPLC) system (Dionex DX 500, Dionex, Idstein, Germany). Carbohydrates were separated on a CarboPac PA1 separation column (250 × 4 mm; Dionex, Idstein, Germany) with 56 mM NaOH as an eluent (flow rate = 1 ml $min^{-1}$). Eluted carbohydrates were detected in an amperometric cell equipped with a gold electrode (Dionex DX 500). Identification and quantification of individual carbohydrates which eluted 8–16 min after injection was done with external standards of sucrose, fructose, and glucose. Peak areas were determined with the PeakNet software (version 5.1, Dionex, Idstein, Germany).

### Analysis of wood composition by FTIR-ATR spectroscopy

Fourier transform infrared spectroscopy–attenuated total reflection (FTIR–ATR) spectra of developing xylem were recorded with an FTIR spectrometer (Equinox 55, Bruker Optics, Ettlingen, Germany) with a deuterium trigylcine sulfate detector and an attached ATR unit (DuraSamplIR, SensIR Europe, Warrington, UK) at a resolution of 4 $cm^{-1}$ in the range from 600 to 4000 $cm^{-1}$.

The bark was peeled off of wood samples before drying so that the uppermost layer of the dried wood consisted of developing xylem. After drying (at 70°C for 7 d) and acclimatization to the measuring room for 24 h, the wood samples were pressed against the diamond crystal of the ATR device; uniform pressure application was ensured using a torque knob. Individual analyses consisted of 32 scans which were averaged to give one spectrum. Each sample was analysed five times in different places, and the five spectra were averaged again, resulting in one mean spectrum per sample. Background scanning and correction were carried out regularly after 10–15 min.

Mean spectra for individual plants were processed using spectroscopy software (OPUS version 6.5, Bruker). A cluster analysis was conducted for the range 1750–1200 $cm^{-1}$ after calculation of first derivatives with nine smoothing points and vector normalization. Compilation of a dendrogram was done by implementing Ward's algorithm (Ward, 1963).

### RNA extraction

Frozen tissue of developing xylem was ground in a ball mill in liquid nitrogen (Retsch). Tissue powder (500 mg) was used for RNA extraction after Chang *et al.* (1993) with minor modifications: the extraction buffer contained 2% β-mercaptoethanol and no spermindine. RNA was purified (RNeasy Mini Kit, Qiagen). Total RNA yield and purity were determined spectrophotometrically (BioPhotometer, Eppendorf, Hamburg, Germany) at $A_{260}$ and $A_{280}$. RNA integrity was assessed on an Agilent 2100 Bioanalyzer (Agilent, Santa Clara, CA, USA) at the Microarray Facility (Tübingen, Germany).

### Microarray analysis and functional annotation

For the control and 100 mM NaCl treatment of both poplar species, three biological replicates were analyzed on a GeneChip® Poplar Genome Array (Affymetrix, Santa Clara, CA, USA). Synthesis of one-cycle cDNA and biotin-labeled cRNA, fragmenting of cRNA, hybridization to the Poplar Genome Array, washing, staining and scanning were performed as stated by Affymetrix (GeneChip® Expression Analysis Technical Manual) at the Microarray Facility, Tübingen. Raw and normalized data are available at the ArrayExpress-database (EMBL:E-MEXP-2031).

To obtain an up-to-date annotation of the microarray probe sets for further analysis, including current Gene Ontology (GO) terms, we performed several steps of BLAST searches (Altschul *et al.*, 1990). The BLAST+ executable from the National Center for Biotechnology Information (NCBI; http://www.ncbi.nlm.nih.gov/) was used to perform a nucleotide BLAST (BLASTn) of the Affymetrix GeneChip Poplar Genome Array target sequences against the Phytozome *Populus trichocarpa* v2.0 transcript database. Gene identifiers (GIs) of the of best hits were retrieved by applying best-hit overhang and best-hit score parameters of 0.1 and 0.05, respectively, as proposed by NCBI in the BLAST Command Line Applications User Manual, and an e-value cutoff of 1E–5. AGI IDs of the closest *Arabidopsis* homologs were determined by a translated nucleotide BLAST (BLASTx) of the coding sequences of the best *P. trichocarpa* hits against the *Arabidopsis thaliana* protein sequence dataset of the representative gene models, applying the same best-hit parameters but a slightly more stringent *e*-value cutoff of 1E–10 to account for cross-species dissimilarities. Annotation details were taken from the latest release of The Arabidopsis Information Resource (TAIR) genome, TAIR10 (November 2010, ftp://ftp.arabidopsis.org/home/tair/Genes/) and the GO TAIR gene association file (release May 2011, http://www.geneontology.org/GO.downloads.annotations.shtml/).

Statistical analysis of the raw signal intensity data of the Affymetrix GeneChips was conducted using the following functions from packages released by the bioconductor project (Gentleman *et al.*, 2004), implemented in R (http://www.r-project.org/).

Background correction, quantile normalization and summarization of the Affymetrix CEL output files were computed using the rma algorithm from the affy package (Irizarry *et al.*, 2003), resulting in a raw list of normalized probe set values. Probe sets referring to genes that were not expressed in the developing xylem were removed by calculating Affimetrix's MAS 5.0 change calls using the mas5calls function from the affy package; only probe sets with three 'present' calls in one of the two treatments were regarded. Also, probe sets for which either no closest *Arabidopsis* homolog was found or no functional annotation was available in the TAIR10 genome release were removed.

Statistical testing for differentially expressed genes and control of the false discovery rate (FDR) was performed on this filtered list of normalized probe set values with a significance analysis of microarrays (SAM) using the 'sam' function from the 'siggenes' package (Tusher *et al.*, 2001). In cases where multiple probe sets corresponded to one gene, duplicates were removed from the list of significant genes by using the Phytozome *P. trichocarpa* GI as a unique identifier; probe sets with the most significant *P*-value were kept for further analysis.

### GO term enrichment analysis and digital northern analysis

For statistical analysis of overrepresented GO terms, a GO term enrichment analysis was conducted using 'The Ontologizer' (Bauer *et al.*, 2008). A GO file for *Populus* was adapted by linking the Phytozome *P. trichocarpa* v2.0 GIs of gene models represented on the Affymetrix GeneChip to the GO identifier of their closest *Arabidopsis* matches as listed in the GO TAIR gene association file. The gene 'population' was defined as the list of filtered probe sets used for the SAM with the Phytozome GI as an unique identifier. 'Study sets' were lists of genes that showed either significantly increased or decreased transcript abundances. As parameter settings, parent–child intersection analysis with Bonferroni correction was used. Graphical outputs were also produced with 'The Ontologizer' using the term-for-term approach with Bonferroni correction. The lists of genes in the 'study sets' were analyzed in PopGenie (http://popgenie.org/) using the tool DigitalNorthern (Sjödin *et al.*, 2009).

### Phylogenetic analysis

For the phylogenetic analysis of the fasciclin-like arabinogalactan-protein (FLA) genes, sequences for open reading frames for *Populus* and *Arabidopsis* were obtained from the Phytozome *P. trichocarpa* v2.0 database and from TAIR. Open reading frames were translated into protein code by GeneDoc (Nicholas *et al.*, 1997) and the resulting amino acid sequences were aligned using Clustal W version 2.0 (Larkin *et al.*, 2007). The unrooted tree was generated using the TreeView program (Page, 1996).

### Validation of microarrays by quantitative real-time polymerase chain reaction (qRT-PCR)

Total RNA was treated with DNAse (Turbo DNA-free kit, Ambion, Austin, TX) and transcribed to cDNA with a RevertAid™ First Strand cDNA Synthesis Kit (MBI Fermentas, St Leon-Rot, Germany). qRT-PCR was performed on an iCycler (Bio-Rad, Hercules, CA, USA) using ABsolute qPCR SYBR Green Fluorescein Mix (ABgene, Surrey, UK). Primer design for the qRT-PCR was performed with the Oligo Explorer and suitable primers were tested for similar melting temperature ($T_m$), primer dimers and primer loops by Oligo Analyzer (both Gene Link, Hawthorne, NY, USA, http://www.genelink.com/). qRT-PCR output was analyzed using the MyiQ software (Bio-Rad). Statistical analysis was conducted using the Pair Wise Fixed Reallocation Randomisation Test (Pfaffl, 2001) implemented in Excel with the Relative Expression Software Tool (REST) – 384 (Pfaffl *et al.*, 2002). qRT-PCR confirmed microarray data (for tested genes, primers and results, see Supporting Information Fig. S1).

## Results

### Osmotic gradient in and ecophysiological responses of *P.* × *canescens* and *P. euphratica* under salt stress

In nonstressed *P.* × *canescens* and *P. euphratica* the difference in the osmotic potential between roots and leaves was approx. $\Delta$ = 0.75 MPa (Fig. 1a,b). When the plants were stepwise acclimated to initially 25 mM NaCl and then to 100 mM NaCl, the osmotic potential of all tissues decreased in *P.* × *canescens*, whereas no significant changes were found in *P. euphratica* (Fig. 1a,b). The strongest decrease in osmotic potential occurred in developing xylem of *P.* × *canescens* and was the result of massive Na accumulation (Fig. 1c). Na accumulation was moderate in *P. euphratica* (Fig. 1d). Previous studies have shown that *P. euphratica* readjusts its internal water balance after exposure to excess salinity within 48 h by a combination of Na accumulation and decreases in K, Ca and sugar concentrations (Ottow *et al.*, 2005; Brinker *et al.*, 2010). Closer inspection of the ion distribution in developing xylem by EDX-SEM revealed that Na accumulation resulted in an approx. fourfold K decrease in *P.* × *canescens*, whereas the reduction in *P. euphratica* was less pronounced (1.5-fold, see Fig. S2).

Salt exposure led to reduced radial growth in *P.* × *canescens*, but not in *P. euphratica* (Table 1). Likewise, only *P.* × *canescens* showed stress symptoms such as leaf senescence (not shown) as well as reductions but not complete abolishment of net $CO_2$ assimilation (Table 1). Despite the decrease in net $CO_2$ assimilation, sugar concentrations in phloem sap of *P.* × *canescens* increased under salt stress (Table 1). In *P. euphratica* neither net $CO_2$ assimilation nor phloem sap carbohydrate concentrations were affected by salt exposure (Table 1). In the developing xylem of 100 mM NaCl-stressed *P.* × *canescens* or *P. euphratica*, no changes in these carbohydrates were found in comparison with controls (not shown).

### Salt stress affects wood anatomy and composition of *P.* × *canescens* and *P. euphratica*

Because salt stress caused a decrease in the osmotic pressure in the xylem of *P.* × *canescens* but not in *P. euphratica*, we anticipated

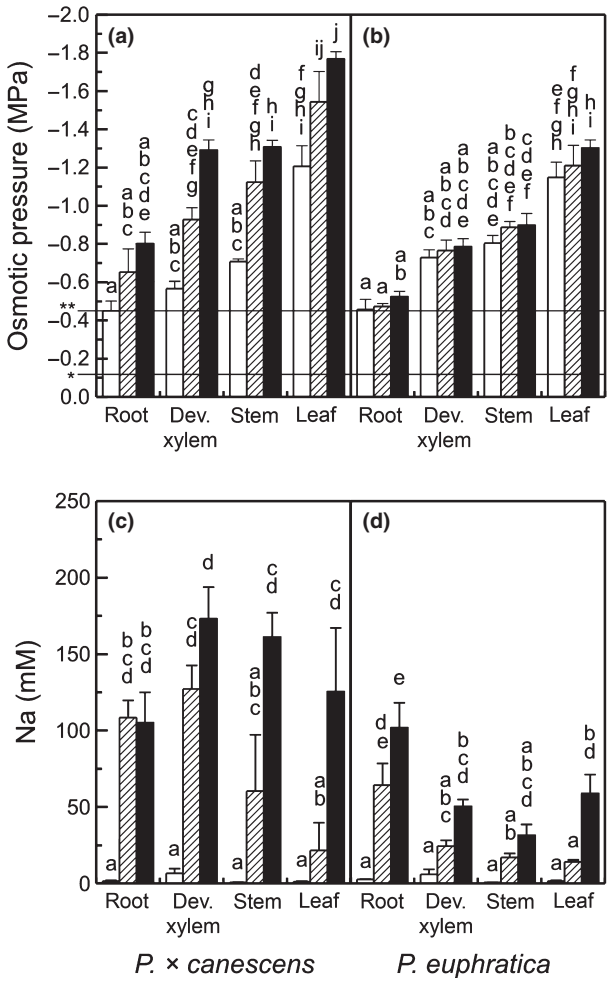


**Fig. 1** Osmotic potentials and sodium concentrations in *Populus* × *canescens* and *Populus euphratica* tissues in response to increasing NaCl concentrations in the nutrient solution. Plants were harvested under control conditions (white), after 2 wk of salt stress with 25 mM NaCl (hatched), and after an additional 2 wk of salt stress with 100 mM NaCl (black). *, osmotic potential of the nutrient solution with 25 mM NaCl; **, osmotic potential of the nutrient solution with 100 mM NaCl. The osmotic potential of the nutrient solution without added NaCl was −0.01 MPa. Osmotic potentials and salt concentrations were calculated based on the water content of the respective tissues. Bars indicate means ± SE ($n$ = 6 (osmolytes), $n$ = 3 (Na), $n$ = 5 (Na in developing (dev.) xylem). Different lower-case letters above bars indicate significant differences at $P \leq 0.05$ obtained by ANOVA followed by a multiple range test (Tukey's honestly significant difference (HSD)).

changes in wood anatomy only in *P.* × *canescens*. As expected, the number of vessels per area increased and the mean vessel diameter decreased from *c.* 31 to 23 μm, resulting in decreasing vessel lumina with increasing salt stress in *P.* × *canescens*, whereas none of these traits was affected in *P. euphratica* (Fig. 2a,b). The predicted hydraulic conductivity computed from vessel frequency and individual sizes of vessel lumina remained constant in both species (Fig. 2c). The changes in frequency and lumen area were limited to the vessels; numbers of fibers and ray cells did not vary in response to salinity (*P.* × *canescens*/*P. euphratica*: number of fibers, 5090/5270 $mm^{-2}$; number of ray cells, 585/580 $mm^{-2}$)

According to the acid-growth theory, cell expansion requires the acidification of the cell walls; protons displace $Ca^{+}$ ions from their linkage positions between pectin molecules, thereby loosening the cell wall (Maggio *et al.*, 2006). We therefore expected that the observed increases in osmotic pressure and growth reductions in salt-stressed *P.* × *canescens* would be accompanied by alkalinization of the cell wall. However, the opposite was observed (Fig. 3). Calibration of the observed changes in color intensity indicated decreases by 0.9 and 0.6 pH units in the developing xylem of salt-exposed *P.* × *canescens* and *P. euphratica*, respectively (Figs S3, S4).

To obtain a chemical fingerprint of the molecular wood composition, FTIR–ATR spectra were measured directly on the surface of the newly formed xylem of *P.* × *canescens* and *P. euphratica* under control conditions and salt stress, respectively (Fig. 4). The spectra showed pronounced differences for the developing xylem of both species and revealed salinity-induced changes in major wood compounds, that is, hemicelluloses (peak 1) and protein (peak 2), lignin (peak 8) and cellulose (peak 6, Fig. 4a). Notably, wood composition of *P. euphratica*, whose anatomy and osmotic potential were not significantly affected, was also influenced by exposure to excess salinity (Fig. 4a). Undirected multivariate analysis showed that the spectra of individual plants formed two main clusters according to species, which were divided into subclusters according to salt treatment (Fig. 4b). The ratios of characteristic wavenumbers showed changes in the lignin : hemicellulose ratio in both poplar species and a significant increase in the lignin : cellulose ratio in *P.* × *canescens* (Table S1). These results indicate that the chemical wood composition, in particular cell wall carbohydrate composition, is responsive to salt exposure and that these changes are uncoupled from or at least precede anatomical changes.

## Transcriptome analysis of developing xylem in *P.* × *canescens* and *P. euphratica* in response to salt stress reveals distinct wood and stress-related regulons

To gain insight into the molecular events associated with the anatomical and compositional changes in poplar wood under salt stress, transcriptional profiles of developing xylem were analyzed on whole-genome microarrays. Genes with significantly changed transcript abundances (differentially expressed genes, DEGs) in response to salt in comparison with untreated controls were determined for each species. The response of the two species differed strongly. In *P.* × *canescens*, a total of 382 genes showed significantly different transcript abundances, but only 39 DEGs were detected in *P. euphratica*. A total of 210 DEGs in *P.* × *canescens* showed increased transcript abundance and 172 showed decreased transcript abundance, while in *P. euphratica* only one gene was up-regulated (Tables S2–S4). Nine DEGs were common to both species, all involved in cell wall metabolism (Table 2).

To detect fundamental patterns underlying the transcriptional changes in *P.* × *canescens*, overrepresented GO categories were determined for DEGs with increased and decreased transcript

**Table 1** Plant performance under salt stress

| Species | Salt treatment NaCl (mM) | Radial growth* (μm $d^{-1}$) | Net $CO_2$ assimilation (μmol $m^{-2}$ $s^{-1}$) | Phloem soluble sugars Glucose (μmol $g^{-1}$ FW) | Fructose (μmol $g^{-1}$ FW) | Sucrose (μmol $g^{-1}$ FW) |
|---|---|---|---|---|---|---|
| *Populus* × *canescens* | 0 | 47.6 (± 7.1) c | 4.58 (± 0.56) b | 9.08 (± 1.45) a | 2.80 (± 0.48) a | 7.07 (± 1.35) a |
| | 25 | 37.9 (± 5.9) b | n.a. | 21.17 (± 4.38) b | 4.70 (± 0.61) b | 18.39 (± 2.25) b |
| | 100 | 13.1 (± 7.1) a | 1.46 (± 0.28) a | 18.43 (± 1.30) b | 3.36 (± 0.26) ab | 21.96 (± 0.87) b |
| *Populus euphratica* | 0 | 15.8 (± 3.1) a | 6.22 (± 1.20) b | 13.22 (± 2.23) a | 2.96 (± 0.31) a | 9.24 (± 0.74) a |
| | 25 | 10.9 (± 3.9) a | n.a. | 14.00 (± 2.15) a | 3.45 (± 0.55) a | 9.96 (± 1.63) a |
| | 100 | 10.5 (± 4.9) a | 5.50 (± 0.23) b | 18.92 (± 5.47) a | 4.72 (± 1.76) a | 12.61 (± 2.07) a |

n.a., not available.
Data are shown for poplars acclimated for 2 wk to 25 mM NaCl or additionally exposed for A further 2 wk to 100 mM NaCl in hydroponic solution and unstressed controls. Data are means of $n = 6$ (± SE). Different letters indicate significant differences at $P < 0.05$. *Radial growth was determined during the last 2 wk before harvest.

abundances, respectively (Table 3). GO terms overrepresented among up-regulated genes in *P.* × *canescens* belonged to the following main categories: 'oxidation-reduction process', 'multi-organism process', 'secondary metabolism', and 'antioxidant activity'. A closer inspection of the enriched GO term hierarchy revealed many defense-related categories (immune response, response to fungus, bacterium, toxin, etc.) and, in addition, also GO terms for 'secondary metabolism' with genes involved in flavonoid and phenylpropanoid metabolism as well as developmental GO terms (e.g. pollen tube guidance) with transcription factors known to regulate cell division (Fig. S5). Overall, these observations support the idea that cell division was still active and radial growth not abolished in response to salt (Table 1).

Among genes with decreased transcript abundance in *P.* × *canescens*, the GO terms 'cell periphery', 'cell wall organization or biogenesis' and 'fluid transport' were overrepresented. Remarkably, the only GO term overrepresented in *P. euphratica* was also 'cell wall organization or biogenesis' (Table 3). In *P.* × *canescens*, the genes annotated by this GO term coded for two plant invertase/pectin methylesterase inhibitors, an expansin-like protein A2, a COBRA-like protein and eight FLAs, and showed the largest overlap (six of 12) with *P. euphratica* (Table 2). Phylogenetic analysis of the related FLA genes from *P. trichocarpa* showed that salt-responsive *FLAs* in *P.* × *canescens* and *P. euphratica* formed a distinct group within subgroup A (subgroup with glycosylphosphatidylinositol (GPI) membrane anchor) with highest similarity with *AtFLA12* (locus At5g60490) (Fig. 5). The over-abundance of *FLAs* was curious because members of this subfamily were massively induced during tension wood formation in poplar (Andersson-Gunneråas *et al.*, 2006). Digital northern analysis employing the DEGs with decreased transcript abundance with poplar libraries available in POPGenie (Sjödin *et al.*, 2009) revealed clustering of 24 and 36% of the salt-repressed DEGs in the cambium and the tension wood libraries, respectively (Fig. 6). By contrast, digital northern analysis of DEGs with increased transcript abundance did not reveal a clear pattern (not shown). This indicates that a suite of genes activated during tension wood formation is collectively suppressed during wood formation under salt stress.

## Discussion

### Salt-induced changes in cell wall composition precede stress responses in the xylem

A remarkable result of this study was the clear distinction of salt responses related to xylem modification and stress adaptation. Transporters putatively involved in salt exclusion were constitutively up-regulated in *P. euphratica* compared with salt-sensitive poplars (Ding *et al.*, 2010; Janz *et al.*, 2010). Here we show that this trait led to exclusion of salt from the above-ground transport path, in particular from the developing xylem. By contrast, highest Na accumulation occurred in the developing xylem of *P.* × *canescens*, consequently requiring strong activation of defenses to prevent injury. In the overrepresented GO term categories for genes with increased transcript abundance typical representatives for osmotic stress as well as for antioxidative defenses were found, for example, genes coding for proteins involved in osmotic adjustment (LEA protein, osmotin precursor, myo-inositol-1-phosphate synthase, trehalose phosphatase), detoxification (glutathione-*S*-transferases, superoxide dismutase, alcohol dehydrogenase) and in signal perception and transduction (ABA-induced protein phosphatase 2C (PP2C), WRKY and MYB transcription factors, the salt responsive homeobox leucin zipper transcription factor HB-7, various serine/threonine protein kinases, 9-cis-epoxycarotenoid dioxygenase involved in ABA biosynthesis) (Table S2). The activation of these genes has also been reported in previous salt screens in roots or leaves of poplar as well as in other plant species (Brosché *et al.*, 2005; Gong *et al.*, 2005; Ottow *et al.*, 2005; Ma *et al.*, 2006; Teichmann *et al.*, 2008; Brinker *et al.*, 2010; Ding *et al.*, 2010; Qiu *et al.*, 2011). Since our plants were acclimated to high salinity and still showed wood formation, this suite of genes must be important to sustain a new degree of cellular homeostasis under stress.

Two GO categories enriched under salt stress in the developing xylem of *P.* × *canescens* deserve specific attention: 'multicellular process' and 'secondary metabolism'. The first category contains a collection of transcription factors involved in cell

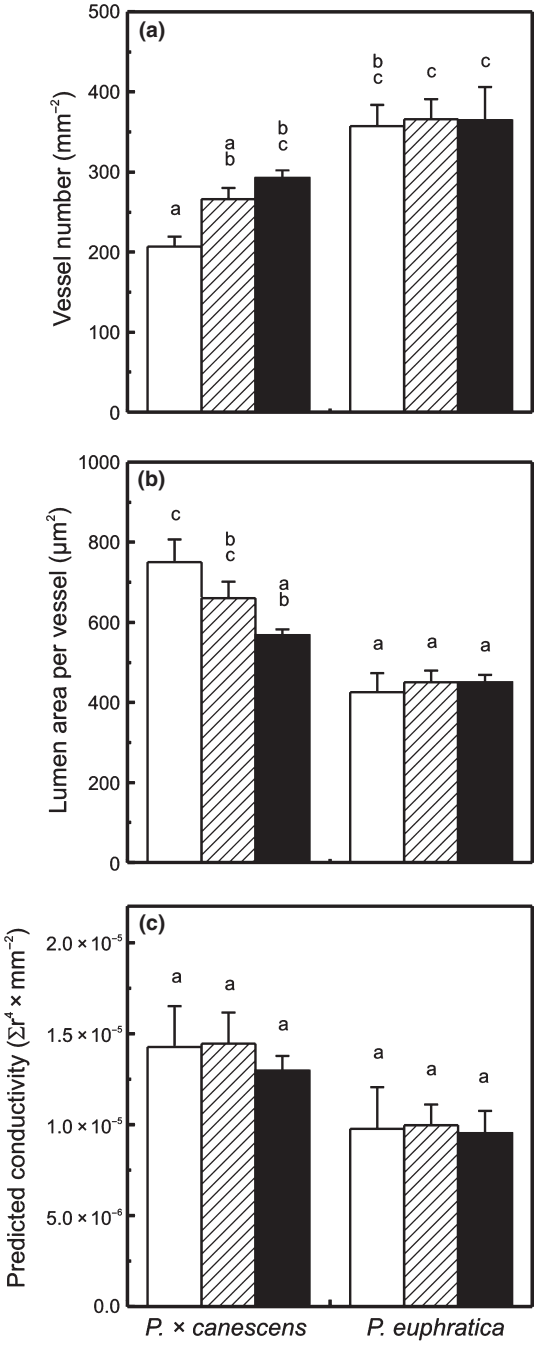


**Fig. 2** Changes in xylem anatomy of *Populus* × *canescens* and *Populus euphratica* in response to salt stress. Plants were harvested under control conditions (white), after 2 wk of salt stress with 25 mM NaCl (hatched), and after an additional 2 wk of salt stress with 100 mM NaCl (black). (a) Number of vessels per cross-sectional area in mm$^2$; (b) mean lumen area of individual vessels in µm$^2$; (c) predicted conductivity, given as the sum of the fourth power radii per area of xylem ($\sum r^4$ mm$^{-2}$). Bars indicate means ± SE ($n$ = 5). Different lower-case letters above bars indicate significant differences at $P \leq 0.05$ obtained by ANOVA followed by a multiple range test (Tukey's honestly significant difference (HSD)).

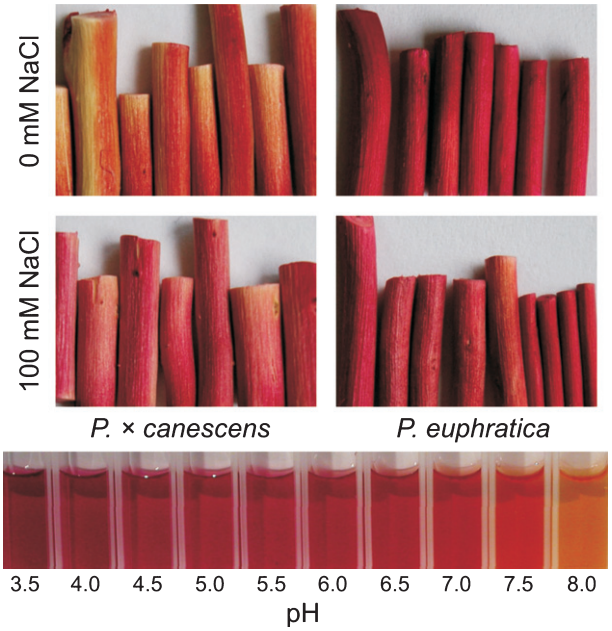


**Fig. 3** pH changes in developing xylem of *Populus* × *canescens* and *Populus euphratica* in response to salt treatment. Stems were debarked and immediately soaked in toluylene red (0.02%). For estimation of the changes in pH value, a calibration series of differing pH values was stained with toluylene red (0.02%). For details see Figs S2, S3.

division and vascular development (e.g. homologs to the *Arabidopsis* genes *KNAT-3* (Truernit *et al.*, 2006) recently identified in *Juglans nigra* during heartwood formation (Huang *et al.*, 2009), *MONOPTEROS* (Ohashi-Ito & Fukuda, 2010), *ANAC087* and *ANAC082* (Guan & Nothnagel, 2004), and *ARF16* (Ding *et al.*, 2010) required for meristem differentiation), thus supporting our cytological and morphometric analyses, which revealed ongoing growth. Significant accumulation of carbohydrates along the transport route (this study) as well as in roots of osmotically stressed poplars (Luo *et al.*, 2009a,b; Galvez *et al.*, 2011) may, however, point to disturbed phloem unloading. Because massive carbohydrate depletion in the developing xylem was not observed, the reasons for the growth reductions remain unclear. Decreased carbon flux to fuel cell wall formation and inhibited vessel expansion by hydraulic stress may have diminished radial growth. It is possible that decreased potassium availability plays a role in this respect (Langer *et al.*, 2002; Wind *et al.*, 2004), but this requires further analyses because it is not clear if elevated concentrations of Na can replace K.

The second category 'secondary metabolism' was not identified in *P. euphratica*. However, this species exhibits constitutive activation of secondary metabolism, even in the absence of salt stress (Janz *et al.*, 2010). Quantitative trait locus (QTL) analyses in poplar progenies revealed that genes for secondary metabolites correlate with drought tolerance (Street *et al.*, 2006). Increased concentrations of flavonoids and phenolics may protect plants against environmental cues because they act as antioxidants preventing cellular injury (Rice-Evans *et al.*, 1997). The pathways for flavonoid production and precursors for lignin (flavonoid 3 hydroxylase, flavonol synthase, flavonol-*O*-methyl transferase, cytochrome P 450 family protein, cinnamoyl CoA reductase, peroxidases) were stimulated in response to salt stress in the developing xylem of *P.* × *canescens*. Substantial increases in lignin relative to cellulose were not detected, suggesting that the production of phenol-based compounds served to increase the

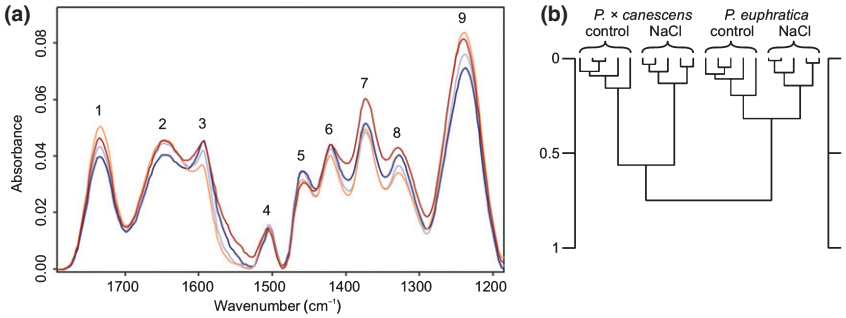


**Fig. 4** Chemical fingerprints of developing xylem from *Populus*. (a) Mean baseline-corrected Fourier transform infrared (FTIR) spectra of developing xylem in the region of wavenumbers from 1200 to 1750 $cm^{-1}$ of *Populus* × *canescens* (red control, orange salt stressed) and *Populus euphratica* (blue, control; cyan, salt-stressed). (b) Cluster analysis of the fingerprint regions of the FTIR spectra. Salt stress was induced by 2 wk of acclimation to 25 mM NaCl and an additional 2 wk of exposure to 100 mM NaCl in the nutrient solution. Spectra are means of five biological replicates. First derivates of spectra after baseline correction were used for cluster analysis using Ward's algorithm and correlation coefficients as distance metrics. Peak numbers in (a) refer to the following molecular components: 1, 1738$cm^{-1}$ = C=O stretch in unconjugated ketones, carbonyls and ester groups in xylans (hemicellulose); 2, 1650$cm^{-1}$ = [a]bsorbed O–H and conjugated C=O of proteins; 3, 1596$cm^{-1}$ = aromatic skeletal vibrations in lignin plus C=O stretch; 4, 1505 $cm^{-1}$ = aromatic skeletal vibrations in lignin plus C=O stretch; 5, 1462 $cm^{-1}$ = C–H deformation; asymmetric in -$CH_3$ and -$CH_2$-; lignin and carbohydrates; 6, 1425 $cm^{-1}$ = aromatic skeletal vibrations combined with C–H plane deformation; lignin and carbohydrates; 7, 1375 $cm^{-1}$ = C–H deformation in cellulose and hemicellulose; 8, 1330$cm^{-1}$ = syringyl ring plus guaiacyl ring condensed; 9, 1235 $cm^{-1}$ = syringyl nuclei deformation combined with deformation of cellulose. Wavenumber assignments were taken from Rana *et al.* (2008) and Zhou *et al.* (2011).

**Table 2** Salt-responsive genes that are common to *Populus* × *canescens* (*P* × *c*) and *Populus euphratica* (*P. eu*) developing xylem and involved in cell wall metabolism

| | | | | Fold change in | |
|---|---|---|---|---|---|
| Affymetrix probe set ID | Phytozome v2.0 GI | AGI | Description | *P* × *c* | *P. eu* |
| PtpAffx.4337.2.S1_at | POPTR_0011s04960 | At4g27450 | Aluminum-induced protein with YGL and LRDR motifs | 0.11 | 0.15 |
| PtpAffx.3761.4.S1_at | POPTR_0008s20870 | At5g18670 | Beta-amylase 3 | 0.44 | 0.21 |
| Ptp.3978.1.S1_at | POPTR_0006s13190 | At2g37130 | Peroxidase superfamily protein | 0.21 | 0.15 |
| Ptp.6380.1.S1_at | POPTR_0004s11620 | At5g15630 | COBRA-like extracellular glycosyl-phosphatidyl inositol-anchored protein family | 0.05 | 0.14 |
| Ptp.3083.1.S1_s_at | POPTR_0009s01730 | At5g60490 | FASCICLIN-like arabinogalactan-protein 12 | 0.04 | 0.20 |
| Ptp.371.2.S1_x_at | POPTR_0013s14780 | At5g60490 | FASCICLIN-like arabinogalactan-protein 12 | 0.14 | 0.19 |
| PtpAffx.142854.1.S1_s_at | POPTR_0012s02220 | At5g60490 | FASCICLIN-like arabinogalactan-protein 12 | 0.23 | 0.21 |
| PtpAffx.162047.1.S1_s_at | POPTR_0009s01740 | At5g60490 | FASCICLIN-like arabinogalactan-protein 12 | 0.07 | 0.18 |
| PtpAffx.33081.1.S1_at | POPTR_0004s22030 | At5g60490 | FASCICLIN-like arabinogalactan-protein 12 | 0.06 | 0.23 |
| Ptp.3500.1.S1_at | POPTR_0012s02210 | At5g60490 | FASCICLIN-like arabinogalactan-protein 12 | 0.27 | nsc |
| Ptp.371.1.S1_at | POPTR_0013s14760 | At5g60490 | FASCICLIN-like arabinogalactan-protein 12 | 0.18 | nsc |
| PtpAffx.249.461.S1_s_at | POPTR_0001s32800 | At5g60490 | FASCICLIN-like arabinogalactan-protein 12 | 0.22 | nsc |
| Ptp.2503.1.S1_at | POPTR_0001s09330 | At5g12250 | Beta-6 tubulin | 0.41 | nsc |
| PtpAffx.202369.1.S1_at | POPTR_0002s19830 | At1g02640 | Beta-xylosidase 2 | 0.27 | nsc |
| Ptp.617.1.S1_at | POPTR_0004s18840 | At4g38400 | Expansin-like A2 | 0.37 | nsc |
| Ptp.4742.2.S1_a_at | POPTR_0019s04700 | At2g39050 | Hydroxyproline-rich glycoprotein family protein | 0.55 | nsc |
| Ptp.4810.1.A1_s_at | POPTR_0003s17450 | At1g04680 | Pectin lyase-like superfamily protein | 0.12 | nsc |
| PtpAffx.211973.1.S1_at | POPTR_0014s17620 | At5g48900 | Pectin lyase-like superfamily protein | 0.30 | nsc |
| PtpAffx.76062.1.A1_s_at | POPTR_0010s16180 | At1g48100 | Pectin lyase-like superfamily protein | 0.17 | nsc |
| Ptp.7635.1.S1_at | POPTR_0014s12180 | At2g47550 | Plant invertase/pectin methylesterase inhibitor superfamily | 0.16 | nsc |
| PtpAffx.140560.1.A1_at | POPTR_0005s06270 | At5g09760 | Plant invertase/pectin methylesterase inhibitor superfamily | 0.30 | nsc |
| PtpAffx.112384.1.S1_at | POPTR_0018s10300 | At4g25810 | Xyloglucan endotransglycosylase 6 | 15.1 | nsc |
| Ptp.5229.1.S1_s_at | POPTR_0007s14570 | At5g65730 | Xyloglucan endotransglucosylase/hydrolase 6 | nsc | 0.07 |
| PtpAffx.107571.1.A1_s_at | POPTR_0001s16270 | At3g14310 | Pectin methylesterase 3 | nsc | 0.08 |

Xylem was harvested from unstressed controls and from trees acclimated for 2 wk to 25 mM and exposed for a further 2 wk to 100 mM NaCl. Complete lists of genes with significantly changed transcript abundances are shown in Tables S2–S4.
nsc, not significantly changed.

antioxidant capacity. It should also be recalled that the FTIR analyses were conducted on the surface of young, not fully differentiated xylem, where lignification was not yet accomplished and therefore the question of whether salt stress led to increased lignin concentrations cannot be conclusively answered yet. However, both species showed changes in cell wall carbohydrates. *P. euphratica* displayed only moderate salt accumulation, which resulted neither in detectable osmotic stress nor in anatomical changes. Our

**Table 3** Enriched Gene Ontology (GO) terms in the lists of differentially expressed genes in developing xylem of *Populus* × *canescens* and *Populus euphratica* under salt stress

| GO ID | Gene ontology | Number of terms in | | Adjusted *P*-value | Direction of change and GO term name |
|---|---|---|---|---|---|
| | | Total population | Study set | | |
| *P.* × *canescens* | | 12604 | 210 | | Genes with increased transcript abundance |
| GO:0055114 | BP | 900 | 41 | 0.000 213 | Oxidation-reduction process |
| GO:0050896 | BP | 3034 | 86 | 0.000 241 | Response to stimulus |
| GO:0051704 | BP | 606 | 29 | 0.000 582 | Multi-organism process |
| GO:0019825 | MF | 50 | 7 | 0.009 975 | Oxygen binding |
| GO:0040011 | BP | 11 | 4 | 0.023 101 | Locomotion |
| GO:0019748 | BP | 229 | 15 | 0.045 592 | Secondary metabolic process |
| GO:0016209 | MF | 63 | 7 | 0.075 101 | Antioxidant activity |
| *P.* × *canescens* | | 12604 | 171 | | Genes with decreased transcript abundance |
| GO:0071944 | CC | 1941 | 51 | 0.000 286 | Cell periphery |
| GO:0071554 | BP | 194 | 12 | 0.004 142 | Cell wall organization or biogenesis |
| GO:0042044 | BP | 30 | 5 | 0.055 002 | Fluid transport |
| *P. euphratica* | | 11 747 | 38 | | Genes with decreased transcript abundance |
| GO:0071554 | BP | 178 | 6 | 0.034 34 | Cell wall organization or biogenesis |

GO terms after Bonferroni correction in mode 'parent–child intersection' are shown.
BP, biological process; MF, molecular function; CC, cellular component.

results indicate that processes involved in cell wall modification are responsive to subtle alterations in hydraulic signals or the ion balance and can clearly be distinguished from cellular defense reactions.

## Changes in xylem anatomy and cell wall composition adapt poplar to hydraulic stress through generation of 'pressure wood'

Osmotic stress causes strong negative xylem pressures, which can lead to cavitation and subsequently to conduit collapse in the xylem (Hacke & Sperry, 2001). Because the integrity of the water transport system is essential for survival under stressful conditions, plants across a vast range of biomes increase their wall strength by decreasing the ratio of vessel lumen to cell wall thickness in response to water limitation (Hacke *et al.*, 2001). This phenomenon is also known as the hydraulic safety principle because single cavitation incidents pose a lower threat when a high number of conduits are available (Zimmermann, 1983; Tyree & Ewers, 1991). Notably, this hydraulic adaptation strategy can also be found when comparing salt-adapted mangrove species (many small vessels) with nonmangrove species (fewer, larger vessels) of the same genus (Janssonius, 1950). Flexible adjustment of vessel lumina to changes in osmotic conditions by salt or drought has also been reported for poplars (Junghans *et al.*, 2006; Arend & Fromm, 2007; Beniwal *et al.*, 2010; Schreiber *et al.*, 2011; this study) and results in formation of false year rings under field conditions (Liphschitz & Waisel, 1970).

A surprising result of our study was that developing xylem undergoing hydraulic adaptation exhibited a coordinated reduction of gene transcripts identified in tension wood formation of poplar (Andersson-Gunnerås *et al.*, 2006). Tension wood is formed on the upper side of the stem in response to gravitational stimuli and is characterized by low lignin content and strong accumulation of cellulose in the fiber lumina (Timell, 1986). Our results show that hydraulic adaptation apparently involves the opposite regulation of a suite of genes required for tension wood formation, namely *FLA*s, *COBRA-like* (homolog to *Arabidopsis COBL4*), and genes encoding xyloglucan endo transglycolyase, pectin methylesterase, pectin lyase, expansin, xylosidase, and amylase. Most of these genes are members of large gene families in poplars. With the exception of the xylosidase gene, members of these gene families were up-regulated in tension wood (Andersson-Gunnerås *et al.*, 2006) and down-regulated here. Conversely, gene expression of the phenylpropanoid pathway was increased here and significantly decreased in tension wood (Andersson-Gunnerås *et al.*, 2006). In tension wood, cellulose biosynthetic genes (*CES*) were increased but suppression of cellulose synthase genes was not found here, although cellulose formation was impaired. Genetic analysis showed that cellulose deposition is under the control of *AtCOB4* in *Arabidopsis* and the ortholog *BC1* in rice (Brown *et al.*, 2005; Sato *et al.*, 2010). The ortholog of these genes, *COBRA-like*, was suppressed in salt-stressed poplar, pointing to suppression of cellulose biosynthesis by transcriptional regulation. Furthermore, the β-amylase 3 gene identified here is a homolog of *Arabidopsis CYT1*, whose failure in knockout mutants resulted in significant decreases in cellulose and accumulation of defense compounds (Lukowitz *et al.*, 2001). Therefore, transcriptional repression of poplar *COBRA-like* and *β-amylase 3* may have caused alterations in cell wall carbohydrate composition.

The only gene with increased transcript abundance in the young xylem of salt-exposed *P. euphratica* encoded a 1-aminocyclopropane-1-carboxylic acid oxidase (ACC oxidase), a gene required for ethylene production. In poplar, ethylene affects the fiber : vessel ratio (Junghans *et al.*, 2004) and fiber extensibility (Qin *et al.*, 2007). Recently, it was shown that ethylene controls tension wood formation (Love *et al.*, 2009). In compression wood of conifers, a strong correlation of increasing lignin : cellulose ratios and ACC oxidase was reported (Plomion *et al.*, 2000),

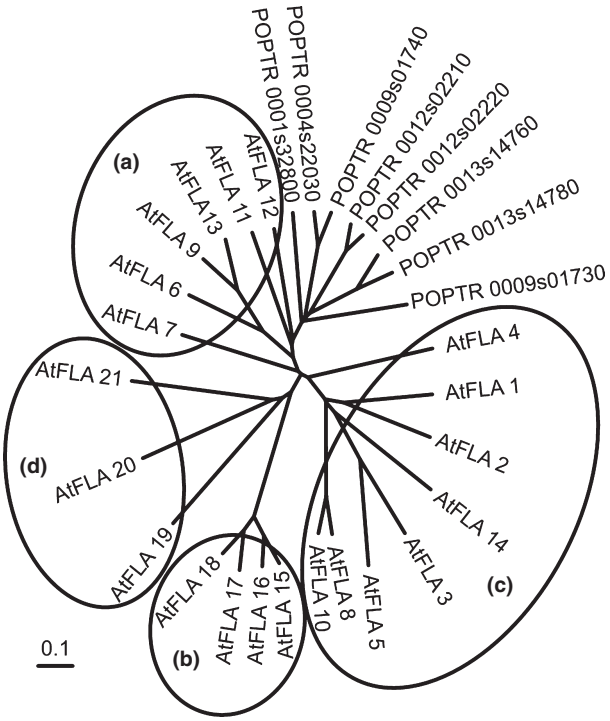


**Fig. 5** Phylogenetic tree of fasciclin-like arabinogalactan proteins (FLAs). Eight closest homologs of *Populus trichocarpa* FLAs to the differentially expressed genes in salt-stressed poplars and the 21 FLA genes in *Arabidopsis* are shown. Phytozome gene identifiers and fold-changes under salt stress are listed in Table 3. AGI locus identifiers for *Arabidopsis* FLAs were obtained from Johnson *et al.* (2003).

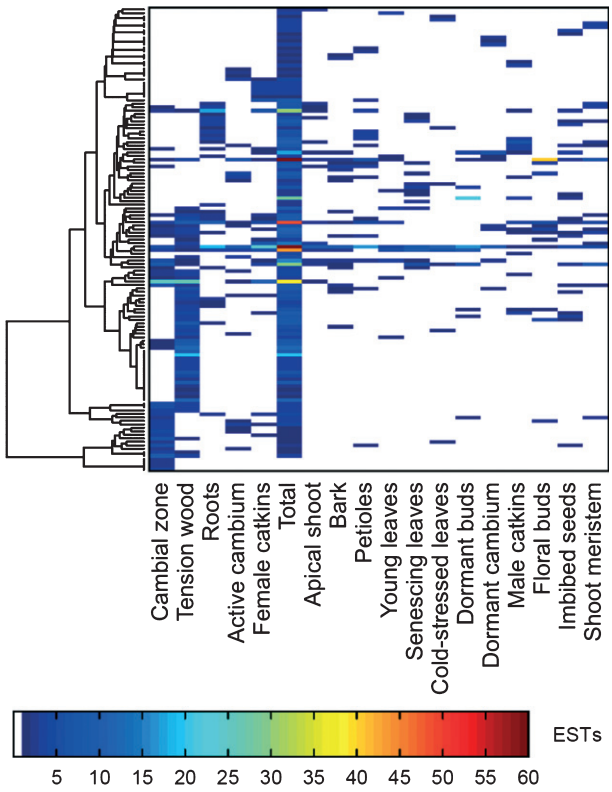


**Fig. 6** Digital northern analysis of genes with decreased transcript abundance after salt stress using expressed sequence tag (EST) libraries for different tissues. The heat map shows the frequencies of genes within EST libraries available at PopGenIE (http://popgenie.org/) that are coregulated with genes with decreased transcript abundance in developing xylem of *Populus* × *canescens* under salt stress.

which might point to a role of ethylene in wood formation under pressure stress.

Fasciclin-like arabinogalactan protein genes (or FLA genes or *FLAs*) are an extremely expanded gene family with several hundred members in poplar (Johnson *et al.*, 2003; Lafarguette *et al.*, 2004; Andersson-Gunneras *et al.*, 2006). The *FLAs* identified as down-regulated in this study form a group of paralogs which have no true orthologs in *Arabidopsis*; this observation has also been made for the *FLAs* massively up-regulated during the formation of tension wood (Andersson-Gunneras *et al.*, 2006). FLAs, which form a distinct subgroup of arabinogalactan-proteins (AGPs), are thought to be involved in various processes of xylem differentiation such as cell–cell signaling, cell division, adhesion, and microfibril orientation and may function as wall integrity sensors affecting downstream signal transduction (Humphrey *et al.*, 2007; Seifert & Blaukopf, 2010). In compression wood of loblolly pine, an *AGP* with GPI anchor (*AGP5*) showed decreased expression (Zhang *et al.*, 2000). The *Arabidopsis* Salt Overly Sensitive 5 (SOS5) protein, a synonym for FLA4 (Swiss-Prot:Q9SNC3), is required for controlled cell expansion (Shi *et al.*, 2003). Phylogenetic comparisons showed that the group A of FLA genes was conserved in monocots and dicots and was specific to stems (MacMillan *et al.*, 2010). Double mutants of *Atfla12/fla11* showed reduced tensile strength and stiffness, thus rendering cell walls more brittle (MacMillan *et al.*, 2010). *Atfla11* and *Atfla12/fla11* mutants also contained lower amounts of cellulose and higher lignin concentrations (Persson *et al.*, 2005; MacMillan *et al.*, 2010). In this study, *P.* × *canescens* and *P. euphratica* showed only a few common reactions towards salt stress; one striking commonality was the suppression of five specific *FLAs* and changes in chemical wood composition resembling those of *Arabidopsis fla* mutants.

We conclude that salinity caused formation of a novel type of 'pressure' wood, presumably as a result of transcriptional coregulation of the same set of genes involved in tension wood biosynthesis, but in the opposite direction. At present, it is mostly unknown how trees sense and signal environmental cues to modify cell walls (Seifert & Blaukopf, 2010). The identification of a putative master relay leading to coordinated stimulation or inhibition of genes for reaction wood formation will be an important research target for future studies.

With regard to practical implications, higher wood density as the result of hydraulic adaptation affects wood biomechanical properties and its technological utilization (Irvine & Grace, 1997; Holtta *et al.*, 2002). Increased lignin : cellulose ratios, as found in compression wood of conifers, have negative effects on pulpability and render such trees less suitable for papermaking (Yeh *et al.*, 2006). However, this wood may be useful as fuelwood for local populations and, therefore, knowledge of the mechanistic basis of wood formed under environmental constraints will help to accelerate the selection of trees that can grow on sodic soils.

## Acknowledgements

We are grateful to S. Wolfart and C. Kettner for excellent technical assistance, to the German Science foundation (DFG) for funding Poplar Research Group Germany (FOR496, Po362/12, Po362/13, Re515/20, Schn653/4) and to the European Commission for supporting parts of this study within the Seventh Framework Program for Research, Project Energypoplar (FP7-211917).

## References

**Abramoff MD, Magelhaes PJ, Ram SJ. 2004**. Image processing with ImageJ. *Biophotonics International* **11**: 36–42.

**Altschul SF, Gish W, Miller W, Myers EW, Lipman DJ. 1990**. Basic local alignment search tool. *Journal of Molecular Biology* **215**: 403–410.

**Amtmann A, Sanders D. 1999**. Mechanisms of $Na^+$ uptake by plant cells. *Advances in Botanical Research Incorporating Advances in Plant Pathology* **29**: 75–112.

**Andersson-Gunneråas S, Mellerowicz EJ, Love J, Segerman B, Ohmiya Y, Coutinho PM, Nilsson P, Henrissat B, Moritz T, Sundberg B. 2006**. Biosynthesis of cellulose-enriched tension wood in *Populus*: global analysis of transcripts and metabolites identifies biochemical and developmental regulators in secondary wall biosynthesis. *Plant Journal* **45**: 144–165.

**Arend M, Fromm J. 2007**. Seasonal change in the drought response of wood cell development in poplar. *Tree Physiology* **27**: 985–992.

**Bauer S, Grossmann S, Vingron M, Robinson PN. 2008**. Ontologizer 2.0 – a multifunctional tool for GO term enrichment analysis and data exploration. *Bioinformatics* **24**: 1650–1651.

**Beniwal RS, Langenfeld-Heyser R, Polle A. 2010**. Ectomycorrhiza and hydrogel protect hybrid poplar from water deficit and unravel plastic responses of xylem anatomy. *Environmental and Experimental Botany* **69**: 189–197.

**Brinker M, Brosche M, Vinocur B, bo-Ogiala A, Fayyaz P, Janz D, Ottow EA, Cullmann AD, Saborowski J, Kangasjarvi J *et al.* 2010**. Linking the salt transcriptome with physiological responses of a salt-resistant *Populus* species as a strategy to identify genes important for stress acclimation. *Plant Physiology* **154**: 1697–1709.

**Brosché M, Vinocur B, Alatalo ER, Lamminmaki A, Teichmann T, Ottow EA, Djilianov D, Afif D, Bogeat-Triboulot MB, Altman A *et al.* 2005**. Gene expression and metabolite profiling of *Populus euphratica* growing in the Negev desert. *Genome Biology* **6**: R101.

**Brown DM, Zeef LAH, Ellis J, Goodacre R, Turner SR. 2005**. Identification of novel genes in *Arabidopsis* involved in secondary cell wall formation using expression profiling and reverse genetics. *Plant Cell* **17**: 2281–2295.

**Chang S, Puryear J, Cairney J. 1993**. A simple and efficient method for isolating RNA from pine trees. *Plant Molecular Biology Reporter* **11**: 113–116.

**Chen S, Polle A. 2010**. Salinity tolerance of *Populus*. *Plant Biology* **12**: 317–333.

**Ding MQ, Hou PC, Shen X, Wang MJ, Deng SR, Sun J, Xiao F, Wang RG, Zhou XY, Lu CF *et al.* 2010**. Salt-induced expression of genes related to $Na^+/K^+$ and ROS homeostasis in leaves of salt-resistant and salt-sensitive poplar species. *Plant Molecular Biology* **73**: 251–269.

**Escalante-Perez M, Lautner S, Nehls U, Selle A, Teuber M, Schnitzler JP, Teichmann T, Fayyaz P, Hartung W, Polle A *et al.* 2009**. Salt stress affects xylem differentiation of grey poplar (*Populus* × *canescens*). *Planta* **229**: 299–309.

**FAO. 2006**. World reference base for soil resources 2006. *World Soil Recourses Reports No. 103. Food and Agriculture Organization of the United Nations.* [WWW document] URL ftp://ftp.fao.org/agl/agll/docs/wsrr103e.pdf [accessed on 15 November 2011].

**Fischer U, Polle A. 2010**. *Populus* responses to abiotic stress. In: Jansson S, Bhalerao R, Groover A, eds. *Genetics and genomics of Populus*. Berlin, Germany: Springer Verlag, 225–247.

**Galvez DA, Landhausser SM, Tyree MT. 2011**. Root carbon reserve dynamics in aspen seedlings: does simulated drought induce reserve limitation? *Tree Physiology* **31**: 250–257.

**Gentleman RC, Carey VJ, Bates DM, Bolstad B, Dettling M, Dudoit S, Ellis B, Gautier L, Ge YC, Gentry J *et al.* 2004**. Bioconductor: open software development for computational biology and bioinformatics. *Genome Biology* **5**: R80.

**Gong QQ, Li PH, Ma SS, Rupassara SI, Bohnert HJ. 2005**. Salinity stress adaptation competence in the extremophile *Thellungiella halophila* in comparison with its relative *Arabidopsis thaliana*. *Plant Journal* **44**: 826–839.

**Guan Y, Nothnagel EA. 2004**. Binding of arabinogalactan proteins by Yariv phenylglycoside triggers wound-like responses in Arabidopsis cell cultures. *Plant Physiology* **135**: 1346–1366.

**Hacke UG, Sperry JS. 2001**. Functional and ecological xylem anatomy. *Perspectives in Plant Ecology Evolution and Systematics* **4**: 97–115.

**Hacke UG, Sperry JS, Pockman WT, Davis SD, McCulloch KA. 2001**. Trends in wood density and structure are linked to prevention of xylem implosion by negative pressure. *Oecologia* **126**: 457–461.

**Heinrichs H, Brumsack HJ, Lotfield N, König N. 1986**. Verbessertes Druckaufschlussystem für biologische und anorganische Materialien. *Zeitschrift für Pflanzenernährung und Bodenkunde* **149**: 350–353.

**Hewitt EJ, Smith TA. 1975**. *Plant mineral nutrition*. London, UK: English U.P.

**Holtta T, Vesala T, Peramaki M, Nikinmaa E. 2002**. Relationships between embolism, stem water tension, and diameter changes. *Journal of Theoretical Biology* **215**: 23–38.

**Huang ZL, Meilan R, Woeste K. 2009**. A KNAT3-like homeobox gene from *Juglans nigra* L., JnKNAT3-like, highly expressed during heartwood formation. *Plant Cell Reports* **28**: 1717–1724.

**Humphrey TV, Bonetta DT, Goring DR. 2007**. Sentinels at the wall: cell wall receptors and sensors. *New Phytologist* **176**: 7–21.

**Irizarry RA, Hobbs B, Collin F, Beazer-Barclay YD, Antonellis KJ, Scherf U, Speed TP. 2003**. Exploration, normalization, and summaries of high density oligonucleotide array probe level data. *Biostatistics* **4**: 249–264.

**Irvine J, Grace J. 1997**. Continuous measurements of water tensions in the xylem of trees based on the elastic properties of wood. *Planta* **202**: 455–461.

**Janssonius H. 1950**. The vessels in the wood of Javan mangrove trees. *Blumea* **6**: 465–469.

**Janz D, Behnke K, Schnitzler JP, Kanawati B, Schmitt-Kopplin P, Polle A. 2010**. Pathway analysis of the transcriptome and metabolome of salt sensitive and tolerant poplar species reveals evolutionary adaption of stress tolerance mechanisms. *BMC Plant Biology* **10**: 150.

**Johnson KL, Jones BJ, Bacic A, Schultz CJ. 2003**. The fasciclin-like arabinogalactan proteins of Arabidopsis. A multigene family of putative cell adhesion molecules. *Plant Physiology* **133**: 1911–1925.

**Junghans U, Langenfeld-Heyser R, Polle A, Teichmann T. 2004**. Effect of auxin transport inhibitors and ethylene on the wood anatomy of poplar. *Plant Biology* **6**: 22–29.

**Junghans U, Polle A, Duchting P, Weiler E, Kuhlman B, Gruber F, Teichmann T. 2006**. Adaptation to high salinity in poplar involves changes in xylem anatomy and auxin physiology. *Plant, Cell & Environment* **29**: 1519–1531.

**Kozlowski TT. 1997**. Responses of woody plants to flooding and salinity. *Tree Physiology Monographs* **1**: 1–29.

**Kundzewicz ZW, Mata LJ, Arnell NW, Döll P, Kabat P, Jiménez B, Miller KA, Oki T, Sen Z, Shiklomanov IA. 2007**. Freshwater resources and their management. In: Parry ML, Canziani OF, Palutikof JP, van der Linden PJ, Hanson CE, eds. *Climate Change 2007: impacts, adaptation and vulnerability. Contribution of Working Group II to the Fourth Assessment Report of the Intergovernmental Panel on Climate Change*. Cambridge, UK: Cambridge University Press, 173–210.

**Lafarguette F, Leple JC, Dejardin A, Laurans F, Costa G, Lesage-Descauses MC, Pilate G. 2004**. Poplar genes encoding fasciclin-like arabinogalactan proteins are highly expressed in tension wood. *New Phytologist* **164**: 107–121.

**Langer K, Ache P, Geiger D, Stinzing A, Arend M, Wind C, Regan S, Fromm J, Hedrich R. 2002**. Poplar potassium transporters capable of controlling $K^+$ homeostasis and $K^+$-dependent xylogenesis. *Plant Journal* **32**: 997–1009.

**Larkin MA, Blackshields G, Brown NP, Chenna R, McGettigan PA, McWilliam H, Valentin F, Wallace IM, Wilm A, Lopez R *et al.* 2007**. Clustal W and clustal X version 2.0. *Bioinformatics* **23**: 2947–2948.

**Leplé JCC, Brasileiro ACM, Michel MF, Delmotte F, Jouanin L. 1992**. Transgenic poplars – expression of chimeric genes using 4 different constructs. *Plant Cell Reports* **11**: 137–141.

**Liphschitz N, Waisel Y. 1970**. The effect of water stresses on radial growth of *Populus euphratica* Oliv. *La Yaaran* **20**: 53–63.

**Love J, Bjorklund S, Vahala J, Hertzberg M, Kangasjarvi J, Sundberg B. 2009**. Ethylene is an endogenous stimulator of cell division in the cambial meristem of *Populus*. *Proceedings of the National Academy of Sciences, USA* **106**: 5984–5989.

**Lukowitz W, Nickle TC, Meinke DW, Last RL, Conklin PL, Somerville CR. 2001**. *Arabidopsis* cyt1 mutants are deficient in a mannose-1-phosphate guanylyltransferase and point to a requirement of N-linked glycosylation for cellulose biosynthesis. *Proceedings of the National Academy of Sciences, USA* **98**: 2262–2267.

**Luo ZB, Janz D, Jiang XN, Gobel C, Wildhagen H, Tan YP, Rennenberg H, Feussner I, Polle A. 2009a**. Upgrading root physiology for stress tolerance by ectomycorrhizas: insights from metabolite and transcriptional profiling into reprogramming for stress anticipation. *Plant Physiology* **151**: 1902–1917.

**Luo ZB, Li K, Jiang XN, Polle A. 2009b**. Ectomycorrhizal fungus (*Paxillus involutus*) and hydrogels affect performance of *Populus euphratica* exposed to drought stress. *Annals of Forest Science* **66**: 106.

**Ma S, Gong Q, Bohnert HJ. 2006**. Dissecting salt stress pathways. *Journal of Experimental Botany* **57**: 1097–1107.

**MacMillan CP, Mansfield SD, Stachurski ZH, Evans R, Southerton SG. 2010**. Fasciclin-like arabinogalactan proteins: specialization for stem biomechanics and cell wall architecture in Arabidopsis and Eucalyptus. *Plant Journal* **62**: 689–703.

**Maggio A, Zhu JK, Hasegawa PM, Bressan RA. 2006**. Osmogenetics: Aristotle to Arabidopsis. *Plant Cell* **18**: 1542–1557.

**Munns R, Tester M. 2008**. Mechanisms of salinity tolerance. *Annual Review of Plant Biology* **59**: 651–681.

**Nicholas KB, Nicholas HB Jr, Deerfield DWI. 1997**. GeneDoc: analysis and visualization of genetic variation. *EMBnet.news* **4**: 1–4.

**Ohashi-Ito K, Fukuda H. 2010**. Transcriptional regulation of vascular cell fates. *Current Opinion in Plant Biology* **13**: 670–676.

**Ottow EA, Polle A, Brosche M, Kangasjarvi J, Dibrov P, Zorb C, Teichmann T. 2005**. Molecular characterization of PeNhaD1: the first member of the NhaD $Na^+/H^+$ antiporter family of plant origin. *Plant Molecular Biology* **58**: 75–88.

**Page RDM. 1996**. TreeView: an application to display phylogenetic trees on personal computers. *Computer Applications in the Biosciences* **12**: 357–358.

**Persson S, Wei HR, Milne J, Page GP, Somerville CR. 2005**. Identification of genes required for cellulose synthesis by regression analysis of public microarray data sets. *Proceedings of the National Academy of Sciences, USA* **102**: 8633–8638.

**Pfaffl MW. 2001**. A new mathematical model for relative quantification in real-time RT-PCR. *Nucleic Acids Research* **29**: e45.

**Pfaffl MW, Horgan GW, Dempfle L. 2002**. Relative expression software tool (REST©) for group-wise comparison and statistical analysis of relative expression results in real-time PCR. *Nucleic Acids Research* **30**: e36.

**Plomion C, Pionneau C, Brach J, Costa P, Bailleres H. 2000**. Compression wood-responsive proteins in developing xylem of maritime pine (*Pinus pinaster* Ait.). *Plant Physiology* **123**: 959–969.

**Qin YM, Hu CY, Pang Y, Kastaniotis AJ, Hiltunen JK, Zhu YX. 2007**. Saturated very-long-chain fatty acids promote cotton fiber and Arabidopsis cell elongation by activating ethylene biosynthesis. *Plant Cell* **19**: 3692–3704.

**Qiu Q, Ma T, Hu QJ, Liu BB, Wu YX, Zhou HH, Wang Q, Wang J, Liu JQ. 2011**. Genome-scale transcriptome analysis of the desert poplar, *Populus euphratica*. *Tree Physiology* **31**: 452–461.

**Rana R, Mueller G, Naumann A, Polle A. 2008**. FTIR spectroscopy in combination with principal component analysis or cluster analysis as a tool to distinguish beech (*Fagus sylvatica* L.) trees grown at different sites. *Holzforschung* **62**: 530–538.

**Rennenberg H, Schneider S, Weber P. 1996**. Analysis of uptake and allocation of nitrogen and sulphur compounds by trees in the field. *Journal of Experimental Botany* **47**: 1491–1498.

**Rice-Evans CA, Miller J, Paganga G. 1997**. Antioxidant properties of phenolic compounds. *Trends in Plant Science* **2**: 152–159.

**Rutledge CB, Douglas GC. 1988**. Culture of meristem tips and micro-propagation of 12 commercial clones of poplar *in vitro*. *Physiologia Plantarum* **72**: 367–373.

**Sato K, Suzuki R, Nishikubo N, Takenouchi S, Ito S, Nakano Y, Nakaba S, Sano Y, Funada R, Kajita S *et al.* 2010**. Isolation of a novel cell wall architecture mutant of rice with defective Arabidopsis COBL4 ortholog BC1 required for regulated deposition of secondary cell wall components. *Planta* **232**: 257–270.

**Schreiber SG, Hacke UG, Hamann A, Thomas BR. 2011**. Genetic variation of hydraulic and wood anatomical traits in hybrid poplar and trembling aspen. *New Phytologist* **190**: 150–160.

**Seifert GJ, Blaukopf C. 2010**. Irritable walls: the plant extracellular matrix and signaling. *Plant Physiology* **153**: 467–478.

**Shi HZ, Kim Y, Guo Y, Stevenson B, Zhu JK. 2003**. The Arabidopsis SOS5 locus encodes a putative cell surface adhesion protein and is required for normal cell expansion. *Plant Cell* **15**: 19–32.

**Sjödin A, Street NR, Sandberg G, Gustafsson P, Jansson S. 2009**. The *Populus* Genome Integrative Explorer (PopGenIE): a new resource for exploring the *Populus* genome. *New Phytologist* **182**: 1013–1025.

**Sperry JS, Meinzer FC, McCulloh KA. 2008**. Safety and efficiency conflicts in hydraulic architecture: scaling from tissues to trees. *Plant, Cell & Environment* **31**: 632–645.

**Street NR, Skogstrom O, Sjodin A, Tucker J, Rodriguez-Acosta M, Nilsson P, Jansson S, Taylor G. 2006**. The genetics and genomics of the drought response in *Populus*. *Plant Journal* **48**: 321–341.

**Teichmann T, Bolu-Arianto WH, Olbrich A, Langenfeld-Heyser R, Gobel C, Grzeganek P, Feussner I, Hansch R, Polle A. 2008**. GH3 :: GUS reflects cell-specific developmental patterns and stress-induced changes in wood anatomy in the poplar stem. *Tree Physiology* **28**: 1305–1315.

**Timell TE. 1986**. *Compression wood in gymnosperms*. Berlin, Germany: Springer.

**Truernit E, Siemering KR, Hodge S, Grbic V, Haseloff J. 2006**. A map of KNAT gene expression in the Arabidopsis root. *Plant Molecular Biology* **60**: 1–20.

**Tusher VG, Tibshirani R, Chu G. 2001**. Significance analysis of microarrays applied to the ionizing radiation response. *Proceedings of the National Academy of Sciences, USA* **98**: 5116–5121.

**Tyree MT, Ewers FW. 1991**. The hydraulic architecture of trees and other woody plants. *New Phytologist* **119**: 345–360.

**Ward JH. 1963**. Hierarchical grouping to optimize an objective function. *Journal of the American Statistical Association* **58**: 236.

**Wind C, Arend M, Fromm J. 2004**. Potassium-dependent cambial growth in poplar. *Plant Biology* **6**: 30–37.

**Yeh TF, Braun JL, Goldfarb B, Chang HM, Kadla JF. 2006**. Morphological and chemical variations between juvenile wood, mature wood, and compression wood of loblolly pine (*Pinus taeda* L.). *Holzforschung* **60**: 1–8.

**Zhang Y, Sederoff RR, Allona I. 2000**. Differential expression of genes encoding cell wall proteins in vascular tissues from vertical and bent loblolly pine trees. *Tree Physiology* **20**: 457–466.

**Zhou GW, Taylor G, Polle A. 2011**. FTIR-ATR-based prediction and modelling of lignin and energy contents reveals independent intra-specific variation of these traits in bioenergy poplars. *Plant Methods* **7**: 9.

**Zimmermann MH. 1983**. *Xylem structure and the ascent of sap*. Berlin, Heidelberg, New York, Tokyo: Springer Verlag.

## Supporting Information

Additional supporting information may be found in the online version of this article.

**Fig. S1** Comparison of qRT-PCR expression and microarray signal ratios.

**Fig. S2** Element analysis of the developing xylem.

**Fig. S3** C/Y-color ratios of a pH-value calibration series.

**Fig. S4** Measured C/Y-color ratios of toluylene-stained wood.

**Fig. S5** Visualization of the relationship of overrepresented GO terms among genes up-regulated in developing xylem of *P.* × *canescens.*

**Table S1** Changes in the chemical composition of developing xylem of *P.* × *canescens* and *P. euphratica* under control conditions and after acclimation to 100 mM NaCl

**Table S2** Genes with significantly higher transcript abundance under salt stress in developing xylem of *P.* × *canescens*

**Table S3** Genes with significantly lower transcript abundance under salt stress in developing xylem of *P.* × *canescens*

**Table S4** Genes significantly differentially expressed under salt stress in developing xylem of *P. euphratica*

Please note: Wiley-Blackwell are not responsible for the content or functionality of any supporting information supplied by the authors. Any queries (other than missing material) should be directed to the *New Phytologist* Central Office.